

# Many-body trial wave functions for atomic systems and ground states of small noble gas clusters

Andrei Mushinski and M.P. Nightingale

Department of Physics, University of Rhode Island, Kingston, Rhode Island 02881

(Received 4 April 1994; accepted 5 August 1994)

Clusters of sizes ranging from two to five are studied by variational quantum Monte Carlo techniques. The clusters consist of Ar, Ne, and hypothetical lighter (" $\frac{1}{2}$ -Ne") atoms. A general form of trial function is developed for which the variational bias is considerably smaller than the statistical error of currently available diffusion Monte Carlo estimates. The trial functions are designed by a careful analysis of long- and short-range behavior as a function of inter-atomic distance; at intermediate distances, on the order of the average nearest neighbor distance, the trial functions are constructed to have considerable variational freedom. A systematic study of the relative importance of  $n$ -body contributions to the quality of the optimized trial wave function is made with  $2 \leq n \leq 5$ . Algebraic invariants are employed to deal efficiently with the many-body interactions.

## I. INTRODUCTION

The experimental and theoretical study of clusters of a variety of sizes and constituents has been pursued vigorously during the last years. Our interest in this field is predominantly motivated by the expectation that it will be possible to perform a detailed comparison of experiments and theoretical predictions obtained by computational physics methods.

In a series of papers various authors have investigated ground and excited state properties of clusters in a wide range of sizes.<sup>1-5</sup> For these studies trial wave functions were used with explicit two- and three-body contributions. In this paper we develop trial wave functions for the ground state of small, bosonic, noble gas clusters. We focus primarily on atoms for which quantum mechanical effects just start to play a role, such as Ar and Ne. Our current goal is to propose and test the quality and numerical tractability of variational forms for the ground state wave functions involving higher-order many-body contributions. The form of these trial functions is derived from that proposed by Umrigar *et al.*<sup>6</sup> for electronic systems, modified to be suitable for systems consisting of identical bosons. Our goal for future work is to use similar trial functions for excited states, where quantum effects are expected to be more pronounced. However, before dealing with this considerably more complex problem, we have chosen to decrease the mass of the atoms as a more practical way of enhancing the quantum mechanical nature of our systems, and therefore, in addition to Ar and Ne, we also studied " $\frac{1}{2}$ -Ne" clusters, which consist of hypothetical atoms with the same inter-atomic potential as Ne, but only half its mass. In this way, for the time being at least, we also avoid the problem that He clusters are expected to have either extremely weakly bound states or no bound states at all for the systems as small as we study.

We use the proposed trial wave functions to obtain variational Monte Carlo estimates of the ground state energy. The quality of the optimized trial wave functions is such that we obtain variational estimates of the ground state energy that in most cases have smaller errors than the diffusion Monte Carlo estimates of Ref. 4, even though the latter, in contrast

to our variational estimates, have no systematic errors.

The layout of this paper is as follows. The formulation of the problem is in Sec. II. Section III contains a discussion of the trial functions. The basic variational form of the trial wave function is derived within the two-body approximation in Sec. III B. Long-distance and short-distance asymptotic properties are discussed in Secs. III B 1 and III B 2. The intermediate-distance range requires most of the variational freedom of the trial function. This is provided by the power series expansion discussed in Sec. III B 3. Trial functions of high quality require many-body contributions. Section III C deals with those, and also with the basis of fundamental polynomial invariants employed as an efficient numerical tool to implement trial functions with Bose symmetry as required for the noble gas clusters we consider. The numerical results, presented in Sec. IV, illustrate the effects of truncation of the intermediate-range power series and of higher-order many-body contributions. Finally, technical details are contained in Appendices A and B. Appendix A describes the Monte Carlo algorithm, trial function optimization, numerical differentiation, and gives optimized parameters of the Ne<sub>3</sub> wave function as an explicit numerical example. The invariants mentioned above are tabulated in Appendix B.

## II. FORMULATION OF THE PROBLEM

The purpose of this paper is to develop and study trial wave functions for ground states of clusters consisting of a small number of identical bosons interacting via a pair potential. The position of the atom  $i$  is given by  $\mathbf{r}_i$  and the distance between atoms  $i$  and  $j$  is denoted by  $r_{ij} = |\mathbf{r}_j - \mathbf{r}_i|$ . As the starting point of our discussion we assume the following dimensionless Hamiltonian for a cluster of  $N$  atoms:

$$H = -\frac{1}{2m} \sum_{i=1}^N \nabla_i^2 + \sum_{(i,j)} V(r_{ij}), \quad (1)$$

where  $(i,j)$  runs over all different pairs of atoms;  $V$  is the dimensionless Lennard-Jones potential

$$V(r) = \frac{1}{r^{12}} - \frac{2}{r^6}. \quad (2)$$

Equations (1) and (2) have been made dimensionless by expressing distances and energies in units of the diameter  $\sigma$  and the well depth  $\epsilon$  of the Lennard-Jones potential, and if  $\mu$  is the atomic mass,  $m^{-1} \equiv \alpha = \hbar^2 / \mu \sigma^2 \epsilon$  is proportional to the square of the de Boer parameter.<sup>7</sup>

Denote by  $\mathbf{R} = (\mathbf{r}_1, \dots, \mathbf{r}_N)$  a  $3N$ -dimensional vector in configuration space and let  $\Psi_T(\mathbf{R}, \mathbf{p})$  be the trial wave function in the coordinate representation, where  $\mathbf{p} = (p_1, p_2, \dots)$  are adjustable parameters. We will omit the arguments of  $\Psi_T$ , where it does not lead to confusion. Following Umrigar *et al.*,<sup>6</sup> we optimize the parameters  $\mathbf{p}$  of the trial wave function by minimizing the variance of the local energy

$$\mathcal{E}(\mathbf{R}, \mathbf{p}) = \frac{1}{\Psi_T} H \Psi_T. \quad (3)$$

If  $\Psi_T$  is the exact ground state of the Hamiltonian, the local energy  $\mathcal{E}$  equals the corresponding eigenvalue of  $\Psi_T$ , independent of  $\mathbf{R}$ . The existence of this zero-variance principle for the ideal case of a true ground state motivates minimization of the variance of the local energy. Of course, the variance vanishes for any eigenstate of the Hamiltonian, but by choosing a strictly positive trial function we can guarantee that in fact we are approximating the ground state rather than an excited state.

In principle, the parameters  $\mathbf{p}$  are determined by minimization of the variance

$$\chi^2(\mathbf{p}) = \frac{\int \Psi_T^* (H - \tilde{E}_0)^2 \Psi_T d\mathbf{R}}{\int |\Psi_T|^2 d\mathbf{R}}, \quad (4)$$

where

$$\tilde{E}_0(\mathbf{p}) = \frac{\int \Psi_T^* H \Psi_T d\mathbf{R}}{\int |\Psi_T|^2 d\mathbf{R}}, \quad (5)$$

the variational estimate of the ground state energy. In practice, minimization of  $\chi^2$ , as given in Eq. (4), is performed with the usual Monte Carlo scheme.<sup>6</sup> (We refer the reader to Appendix A for details of the algorithm and its efficient implementation.)

We define a quantitative measure  $Q$  of the quality of a trial wave function  $\Psi_T$  as

$$Q = -\log_{10} \frac{\chi}{|E_0|}, \quad (6)$$

where the limit  $Q \rightarrow \infty$  corresponds to an *exact* solution of the time-independent Schrödinger equation. In terms of the quality  $Q$ , one can estimate the intrinsic error of the variational energy  $\tilde{E}_0$ . The difference between an exact ground state energy  $E_0$  and the variational estimate  $\tilde{E}_0$  is bounded by  $\chi$ :

$$\tilde{E}_0 - \chi \leq E_0 \leq \tilde{E}_0. \quad (7)$$

(This inequality and the next one are reviewed in Ref. 8.) If one knows the energy  $E_1$  of the lowest excited state of the same symmetry as the trial wave function, a lower bound can be obtained that is tighter for sufficiently small  $\chi^2$ , viz.,

$$\tilde{E}_0 - \frac{\chi^2}{|E_1 - E_0|} \leq E_0 \leq \tilde{E}_0. \quad (8)$$

Use of Eqs. (7) and (8)  $E_0$  implicitly makes the assumption that the trial wave function approximates the ground state, rather than an excited state, an assumption that is justified on physical grounds.

The relative error in the energy expressed in terms of this last inequality (8) can be measured by

$$Q' = -\log_{10} \frac{\chi^2}{(E_1 - E_0)|E_0|}. \quad (9)$$

In estimates of  $Q$  in Eq. (6) we replace  $E_0$  by the variational estimate  $\tilde{E}_0$ ; in the case of  $Q'$ , we also replace  $E_1 - E_0$  in Eq. (9) by the approximate gap obtained from the rather crude, harmonic approximation.

### III. TRIAL WAVE FUNCTIONS

#### A. Symmetries

A trial wave function for the ground state of a bosonic noble gas cluster should be invariant under translation, rotation, and particle permutation. We satisfy the first two of these requirements by choosing as our coordinates the interatomic distances  $r_{ij}$ ,  $1 \leq i < j \leq N$ . This set of coordinates has  $\frac{1}{2} N(N-1)$  elements rather than the required minimal number of  $\max(3N-6, 1)$  and since the former exceeds the latter for  $N \geq 5$ , there will be dependences among the interparticle distances in that case. However, these dependences will automatically be satisfied because the  $r_{ij}$  will only assume values derived from configurations given by the  $3N$  variables  $\mathbf{R}$ . The third condition, particle exchange symmetry, has to be imposed explicitly by considering only those functions that are invariant under permutation of the indices of all  $r_{ij}$ .

In addition to these symmetry restrictions, we impose the condition of positivity on the trial function. In principle,  $n$ -body correlations with all  $n \leq N$ , should be incorporated in the trial wave function, but these many-body effects are expected to become progressively less important as  $n$  increases. Positivity and many-body correlations suggest that the trial function be written as

$$\log \Psi_T = \sum_{(i,j)} u^{(2)}(r_{ij}) + \sum_{(i,j,k)} u^{(3)}(r_{ij}, r_{jk}, r_{ki}) + \dots + \sum_{(i_1, \dots, i_N)} u^{(N)}(r_{i_1 i_2}, \dots), \quad (10)$$

where the  $u^{(n)}$  are real-valued,  $n$ -body functions.

#### B. Two-body approximation

The symmetries discussed above are not the only restrictions on the form of the wave function given in Eq. (10). Further restrictions are derived from the asymptotic behavior of the local energy for some particular cases of the  $r_{ij} \rightarrow 0$  and  $r_{ij} \rightarrow \infty$  limits. For the  $r_{ij} \rightarrow 0$  limit we consider the special case where the pair distance  $r_{ij}$  of one arbitrary pair vanishes, while all other pair distances remain finite and non-zero. Collisions involving more than two particles impose

additional asymptotic conditions on the wave function, but these are presumably less important and will be ignored. Also in the  $r_{ij} \rightarrow \infty$  limit we restrict ourselves to a special case: one particle goes off to infinity, while all others stay fixed.

First we derive the expression for the local energy using the two-body approximation to the wave function, i.e.,

$$\log \Psi_T = \sum_{(i,j)} u^{(2)}(r_{ij}). \quad (11)$$

The general expression for the local energy is

$$\mathcal{E} = -\frac{\alpha}{2} \sum_{i=1}^N [\nabla_i^2 \log \Psi_T + (\nabla_i \log \Psi_T)^2] + \sum_{(i,j)} V(r_{ij}). \quad (12)$$

For a trial wave function with only two-body correlations this equation reduces to

$$\mathcal{E} = -\frac{\alpha}{2} \sum_i \left[ \sum_{j \neq i} u'(r_{ij}) \mathbf{e}_{ij} \right]^2 - \alpha \sum_{(i,j)} \left[ u''(r_{ij}) + \frac{2}{r_{ij}} u'(r_{ij}) \right] + \sum_{(i,j)} \left[ \frac{1}{r_{ij}^{12}} - \frac{2}{r_{ij}^6} \right], \quad (13)$$

where  $u'$  and  $u''$  denote first- and second-order derivatives of  $u^{(2)}$ ;  $\mathbf{e}_{ij}$  denotes the unit vector  $(\mathbf{r}_j - \mathbf{r}_i)/r_{ij}$ .

The current approximation to the wave function contains no explicit three-body correlations, yet the local energy contains three-body contributions as shown explicitly by rewriting Eq. (13) in the following form

$$\mathcal{E} = \mathcal{E}^{(2)} + \mathcal{E}^{(3)} = \sum_{(i,j)} \mathcal{E}_{ij} + \sum_{(i,j,k)} \mathcal{E}_{ijk}, \quad (14)$$

where

$$\mathcal{E}_{ij} = -\alpha \left[ u''(r_{ij}) + \frac{2}{r_{ij}} u'(r_{ij}) + u'^2(r_{ij}) \right] + \left( \frac{1}{r_{ij}^{12}} - \frac{2}{r_{ij}^6} \right) \quad (15)$$

is local energy of a pair, and where, writing  $\mathbf{u}_{ab} \equiv u'(r_{ab})\mathbf{e}_{ab}$ , one has

$$\mathcal{E}_{ikm} = \alpha(\mathbf{u}_{ki} \cdot \mathbf{u}_{im} + \mathbf{u}_{ik} \cdot \mathbf{u}_{km} + \mathbf{u}_{im} \cdot \mathbf{u}_{mk}), \quad (16)$$

which is the "connected" local energy of a triplet, i.e., the contribution to the local energy not accounted for by pair contributions.  $\mathcal{E}^{(3)}$  in Eq. (14) can be rewritten in terms of two-particle interactions mediated by all other particles:

$$\mathcal{E}^{(3)} = \alpha \sum_{(ij)} \sum_{p \neq i,j} \mathbf{u}_{ip} \cdot \mathbf{u}_{pj}. \quad (17)$$

## 1. Long-distance behavior

To derive the asymptotic properties at infinity we consider configurations in which one atom goes off to infinity while the others remain fixed. Equations (11) and (13) show that the conditions, first, that the local energy remain finite, and, second, that the atoms in the cluster be in a bound state, imply that  $u'(r)$  approaches a real, negative constant for  $r \rightarrow \infty$ .

## 2. Short-distance behavior

As is well-known, good trial functions for electron systems satisfy the "cusp" condition,<sup>9</sup> which guarantees that for two-body collisions the contribution to the local energy due to the divergent electron-electron (or electron-nucleus) Coulomb potential energy is canceled by a divergence of opposite sign in the kinetic energy. Analogously, as a first step in dealing with the divergence in  $\mathcal{E}$  at short distances for the case of the Lennard-Jones potential, we suppose that one pair distance, say  $r_{12}$ , is small compared to unity and all other pair distances. Then the dominant contributions to  $\mathcal{E}$  in Eq. (13) come from the divergences at  $r_{12}=0$ , and if one keeps only terms that contain  $r_{12}$ , the singular part of  $\mathcal{E}$  can be approximated as a function of only the one argument  $r \equiv r_{12}$ :

$$\mathcal{E} \approx -\alpha u''(r) - 2\alpha \left( \frac{1}{r} + \xi \right) u'(r) - \alpha u'^2(r) + \frac{1}{r^{12}} - \frac{2}{r^6}, \quad (18)$$

where  $\xi$  plays the role of a "random field" associated with the positions of particles 3,...,N:

$$\xi = -\frac{1}{2} \sum_{i>2} [u'(r_{i1})\mathbf{e}_{21} \cdot \mathbf{e}_{1i} + u'(r_{2i})\mathbf{e}_{12} \cdot \mathbf{e}_{2i}], \quad (19)$$

a field that vanishes only for a diatomic cluster.

We choose

$$u'(r) = b_{-6}/r^6 + b_{-1}/r + b_0 + b_4 r^4 + b_5 r^5 + O(r^6) \quad (20)$$

with coefficients to be determined to cancel the short-distance divergences in the local energy. For the local energy this yields

$$\begin{aligned} \mathcal{E}(r) = & \frac{1 - \alpha b_{-6}^2}{r^{12}} - \frac{2\alpha b_{-6}(b_{-1} - 2)}{r^7} - \frac{2\alpha b_{-6}(b_0 + \xi) + 2}{r^6} \\ & - \frac{\alpha(2b_{-6}b_4 + b_{-1} + b_{-1}^2)}{r^2} \\ & - \frac{2\alpha(b_0 + b_{-6}b_5 + b_{-1}b_0 + b_{-1}\xi)}{r} \\ & - \alpha b_0(b_0 + 2\xi) - 2\alpha b_4(3 + b_{-1})r^3 + O(r^4). \end{aligned} \quad (21)$$

The following choice of the  $b_i$  for a given value of the random field  $\xi$  eliminates the power law divergences:

$$\begin{aligned} b_{-6} &= \frac{1}{\sqrt{\alpha}}, \quad b_{-1} = 2, \quad b_0 = -\frac{1}{\sqrt{\alpha}} - \xi, \\ b_4 &= -3\sqrt{\alpha}, \quad b_5 = 3 + \sqrt{\alpha}\xi. \end{aligned} \quad (22)$$

With the  $b_i$  as given in Eqs. (22), the  $r^{-12}$ ,  $r^{-7}$ , and  $r^{-2}$  divergences in the local energy in Eq. (21) are eliminated simultaneously for all configurations of the  $N$  atoms. However, since the expressions for  $b_0$  and  $b_5$  depend on the random field  $\xi$ , the best one can do with the remaining  $r^{-6}$  and  $r^{-1}$  divergences is to have their amplitudes vanish in an average sense. For the local energy this particular choice, i.e., replacing  $\xi$  by its average value, yields

$$\mathcal{E}(r) = -\frac{2\sqrt{\alpha}\eta}{r^6} - \frac{4\alpha\eta}{r} - [(1 - \sqrt{\alpha}\eta)^2 - \alpha\xi^2] + 30\alpha^{3/2}r^3 + O(r^4), \quad (23)$$

with  $\eta \equiv \xi - \langle \xi \rangle$ . Many of the papers mentioned in the introduction contain trial functions with singularities as in Eq. (20) and employ these both for the Lennard-Jones and the Aziz potentials. The main difference is that in the derivation given above the coefficients assume fixed values, while the nature of the terms is determined to cancel divergences explicitly associated with the Lennard-Jones potential. In our approach other potentials would require different terms.

### 3. Intermediate-distance behavior

The behavior of the trial function at distances of most physical significance, distances of order unity, is conveniently expressed in terms of a polynomial. In order to avoid the problem that high-order polynomial terms dominate the behavior of the pair correlation function  $u^{(2)}$  at infinity, we introduce a new (shifted) distance variable  $\hat{r}$  which approaches a constant for  $r \rightarrow \infty$ :

$$\hat{r}(r) = w[1 - e^{(r_0 - r)/w}]. \quad (24)$$

Here  $w$  and  $r_0$  in principle are variational parameters. In practice, the quality of the wave function depends only weakly on their values. They are set to values of order unity and kept fixed during the optimization of the trial function, which allows us to greatly improve the efficiency of the optimization algorithm, as explained in detail in Appendix A. The parameter  $w$  is chosen to reflect the length scale on which correlations exist in the cluster. It should be noted that for values of  $w \gg 1$  the optimization based on a sample of states generated by Monte Carlo (cf. Appendix A) becomes unstable, since the trial function develops too much variational freedom in regions of configuration space associated with cluster conformations of very low probability. The shift  $r_0$  is included for the purpose of numerical accuracy, so that high powers of  $\hat{r}$  assume small values.

In terms of this new variable  $\hat{r}$  we can combine all required behaviors discussed above, by choosing the following variational expression for  $u^{(2)}$  for the trial function:

$$u^{(2)}(r) = -\frac{1}{5r^5\sqrt{\alpha}} - \frac{\gamma r}{\sqrt{\alpha}} + 2 \ln r + \sum_{p=1}^P c_p \hat{r}^p. \quad (25)$$

This form, with  $\gamma$  and the  $c_i$  as variational parameters, provides the required variational freedom for the trial function at intermediate distances, while it also displays the asymptotic behavior derived above for small and large distances. Note that Eq. (25) corresponds to keeping the parameters  $b_i$  with  $i \geq 0$  as free parameters, rather than fixing their values by the expressions given in Eq. (22).

### C. Many-body approximation

The quality of a trial function obtained by exponentiation of the sum over pairs of  $u^{(2)}(r_{ij})$ , as given in Eq. (25), cannot be increased arbitrarily by increasing the degree  $P$  of the polynomial in  $\hat{r}$ . At some point, the effect of the presence

of high-order two-body terms in the polynomial becomes smaller than the effect of the absence of three-body contributions. In principle, one has to allow for  $n$ -body interactions with  $n \leq N$ , and for this purpose we add polynomials in all variables  $\hat{r}_{ij}$  ( $i < j$ ), defined in terms of the original interatomic distances as in Eq. (24). The general form of these  $n$ -body polynomials for  $n > 2$  is

$$u^{(n)} = \sum_{p=0}^P \sum_{\substack{0 \leq p_{12}, p_{13}, \dots, p_{N-1,N} \leq P \\ p_{12} + p_{13} + \dots + p_{N-1,N} = p}}' C_{p_{12}, p_{13}, \dots, p_{N-1,N}} \times \hat{r}_{12}^{p_{12}} \hat{r}_{13}^{p_{13}} \dots \hat{r}_{N-1,N}^{p_{N-1,N}}, \quad (26)$$

where the prime on the summation indicates that the exponents  $p_{ij}$  should be chosen consistent with the condition that  $u^{(n)}$  represent an  $n$ -body interaction; that is, the set of indices  $i$  for which a  $j$  exists such that  $p_{ij} \neq 0$  contains precisely  $n$  elements. Since we are dealing with Bosons, the wave function should be symmetric under particle permutation, i.e.,  $C_{p_{12}, p_{13}, \dots, p_{N-1,N}} = C_{p'_{12}, p'_{13}, \dots, p'_{N-1,N}}$  if  $\hat{r}_{12}^{p_{12}} \hat{r}_{13}^{p_{13}} \dots \hat{r}_{N-1,N}^{p_{N-1,N}} = \hat{r}_{12}^{p'_{12}} \hat{r}_{13}^{p'_{13}} \dots \hat{r}_{N-1,N}^{p'_{N-1,N}}$  and  $\hat{r}_{12}^{p_{12}} \hat{r}_{13}^{p_{13}} \dots \hat{r}_{N-1,N}^{p_{N-1,N}}$  can be obtained from each other by a particle permutation.

Dealing explicitly with the particle permutation symmetry for general  $n$ -body interactions in the context of polynomials of the form of Eq. (26) is rather cumbersome from the point of view of programming, and also computationally expensive. As an alternative, we constructed, for each cluster size  $N$ , a basis of  $M$  fundamental polynomial invariants  $I_{N1}, \dots, I_{NM}$ .<sup>10</sup> In terms of the basis formed by the  $I_{Nk}$  one can conveniently express all polynomials in the variables  $\hat{r}_{12}, \hat{r}_{13}, \dots$  that are symmetric under all permutations of indices. Each fundamental invariant  $I_{Nk}$  can be chosen to be a homogeneous, permutationally symmetric polynomial of degree  $d_k$  in the variables  $\hat{r}_{ij}$ . Expressed in terms of these fundamental invariants, the logarithm of the trial function reads

$$u(\mathbf{R}) = - \sum_{(ij)} \left( \frac{1}{5\sqrt{\alpha}r_{ij}^5} + \frac{\gamma r_{ij}}{\sqrt{\alpha}} - 2 \ln r_{ij} \right) + \sum_{\substack{q_1, q_2, \dots, q_M \\ q_1 d_1 + q_2 d_2 + \dots + q_M d_M \leq P}} C_{q_1, \dots, q_M} I_{N1}^{q_1} \dots I_{NM}^{q_M}. \quad (27)$$

As a simple example we discuss the case of a three particle cluster. For  $N=3$  a possible classic choice for a basis of fundamental invariants is

$$I_{31} = \hat{r}_{12} + \hat{r}_{23} + \hat{r}_{13}, \quad I_{32} = \hat{r}_{12}^2 + \hat{r}_{23}^2 + \hat{r}_{13}^2, \quad I_{33} = \hat{r}_{12}\hat{r}_{23}\hat{r}_{13}. \quad (28)$$

Fundamental invariants for the cases of three, four, and five particles are given in Appendix B.

We end this section with a few comments regarding the efficiency of employing a basis of fundamental invariants. The number of terms of a polynomial in  $v$  variables of order  $P$  is given by the binomial coefficient  $\binom{v+P}{P}$ . This implies that for a five atom cluster the full many-body polynomial of

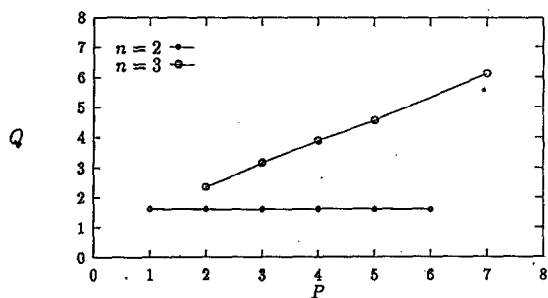


FIG. 1. Quality  $Q$ , a measure of the accuracy of the optimized trial function as defined in Eq. (6), as a function of the power  $P$  of two- and three-body polynomials, labeled by  $n$ , for  $\text{Ar}_3$ .

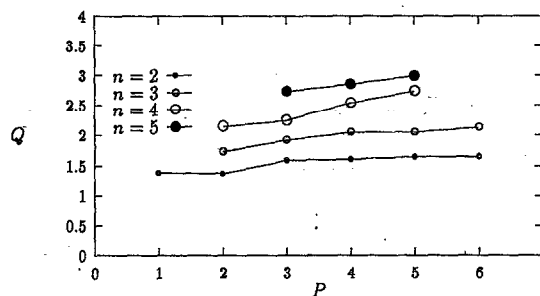


FIG. 3. Quality  $Q$ , a measure of the accuracy of the optimized trial function as defined in Eq. (6), as a function of the power  $P$  of two-, three-, four- and five-body polynomials, labeled by  $n$ , for  $\text{Ar}_5$ .

degree five in the ten variables  $\hat{r}_{ij}$  ( $1 \leq i < j \leq 5$ ) has 3003 terms, if all possible many-body interactions and a constant are included. If one evaluates such a polynomial by recursively applying Horner's rule to all variables this requires 3003 multiplications, which we shall take as the measure of the computational effort. Of course, this approach would also require a scheme of equating polynomial coefficients to impose the restriction to polynomials of the required symmetry.

Written as a polynomial in the fundamental invariants listed in Appendix B there are only 64 terms. Since the evaluation of the invariants given in Appendix B takes about 700 multiplications, use of invariants speeds up the calculation by a factor almost equal to four, a number that might be improved since we made no systematic attempt to optimize the numerical efficiency of the bases of fundamental invariants.

Simple use of Horner's rule applied recursively to the variable  $\hat{r}_{12}, \hat{r}_{13}, \dots$ , makes no use at all of the Boson symmetry of the polynomial. As an alternative to employing a basis of fundamental invariants, the particle permutation symmetry can be exploited by constructing the terms in the polynomial diagrammatically. This has the advantage of providing naturally a separation of the polynomial in contributions separated into  $n$ -body terms sorted according to different values of  $n$ . For  $N=P=5$  example discussed above the

use of collecting and factorizing terms diagrammatically reduces the effort by about a third compared to the brute force approach using Horner's rule.

These considerations apply to the case of one single evaluation of the trial wave function, but in practice this is not always the operation of interest. For example, during the optimization phase one only has to compute the change in a trial function that results from the change in the variational parameters (see Appendix A). For a variational or diffusion Monte Carlo calculation what may matter is the change of the wave function in response to a change of the coordinates of just one atom. In such cases the increase in speed associated with the use of invariants may be even greater.

In its simplest implementation use of invariants mixes up all many-body interactions and destroys the separation into  $n$ -body interactions for different values of  $n$  and the hierarchy as implied in Eq. (10). There is a solution to this problem, but we have not yet explored it in detail nor is it relevant within the limited scope of this paper.

#### IV. NUMERICAL RESULTS

Our first numerical results address how much accuracy is gained in the quality of the trial wave function as  $n$ -body terms with progressively larger values of  $n$  are included. Figures 1–3 display results for argon clusters of sizes three,

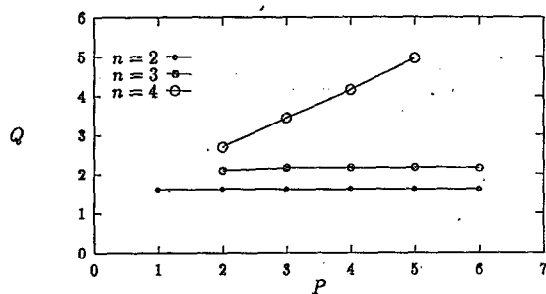


FIG. 2. Quality  $Q$ , a measure of the accuracy of the optimized trial function as defined in Eq. (6), as a function of the power  $P$  of two-, three- and four-body polynomials, labeled by  $n$ , for  $\text{Ar}_4$ .

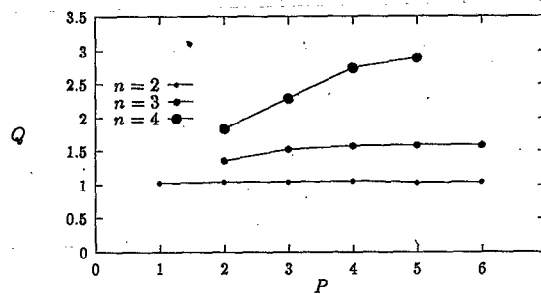


FIG. 4. Quality  $Q$ , a measure of the accuracy of the optimized trial function as defined in Eq. (6), as a function of power  $P$  of two-, three- and four-body polynomials, labeled by  $n$ , for  $\text{Ne}_4$ .

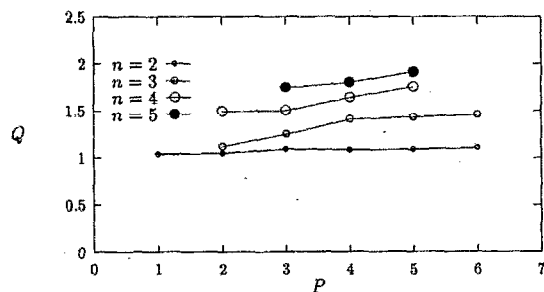


FIG. 5. Quality  $Q$ , a measure of the accuracy of the optimized trial function as defined in Eq. (6), as a function of power  $P$  of two-, three-, four- and five-body polynomials, labeled by  $n$ , for  $\text{Ne}_5$ .

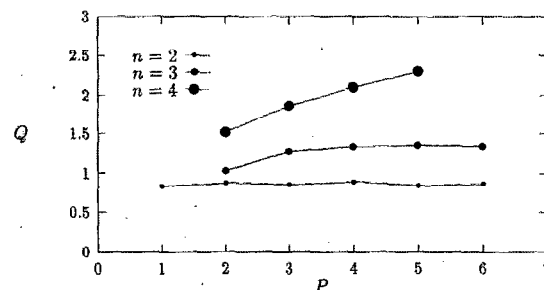


FIG. 7. Quality  $Q$ , a measure of the accuracy of the optimized trial function as defined in Eq. (6), as a function of power  $P$  of two-, three- and four-body polynomials, labeled by  $n$ , for  $\frac{1}{2}\text{-Ne}_4$ .

four, and five.  $Q$ , our most conservative estimate of the quality of the wave functions as defined in Eq. (6), is plotted versus the power  $P$  of the polynomials defined in Eqs. (25) and (26), for different values of  $n$ . The bottom curve, starting at  $P=1$ , is for the case in which only two-body interactions are present ( $n=2$ ). As shown, the quality levels off at a fixed value of  $Q$  with increasing  $P$ , an indication that in that regime the absence of three-body terms in the logarithm of the trial wave function is the dominant source of the variance of the local energy. In the next curve segment three-body terms are added ( $n=3$ ). Here  $P$  is redefined to denote the order of three-body polynomial, which starts at  $P=2$ ; in the second curve segment the order of the polynomial that describes two-body effects is kept constant at the highest  $P$ -value used in the previous segment of the curve. This process is repeated for  $n$ -body terms with increasing  $n$  until finally the complete  $N$ -body polynomial for the  $N$ -atom cluster is included in the trial function. At this point, the quality starts to go up roughly linearly with the order of the polynomial. Note, however, that the order  $P$  of the four-body polynomials is not sufficiently high in any of the figures for the quality to have leveled off, as ultimately it must. Analogous plots for  $\text{Ne}_4$  and  $\text{Ne}_5$  are shown in Figs. 4 and 5, and for  $\frac{1}{2}\text{-Ne}_3$ ,  $\frac{1}{2}\text{-Ne}_4$ , and  $\frac{1}{2}\text{-Ne}_5$  are shown in Figs. 6–8. Figures 9–11

display plots of the quality  $Q$  vs the power  $P$  for each type and size of cluster for optimized wave functions including the full many-body polynomials. An interesting feature of these plots is that the  $Q$  vs  $P$  curves for three- and four-atom ( $N=3,4$ ) clusters almost coincide but that they are distinct from the curves for  $N=2$  and  $N=5$ . The  $N=2$  clusters are unique in that the short-distance divergences in the local energy have been fully removed [note that  $\eta=0$  in Eq. (23) only for  $N=2$ ], while also the large-distance asymptotic properties of the trial function is superior in this case. Apart from this, the effect probably is geometric in nature: clusters of sizes  $N \leq 4$  are fully symmetric in the classical configuration of minimum energy and can be characterized by a single inter-atomic distance. For  $N=5$  the cluster is frustrated: the classical ground state is a trigonal bipyramid (the faces of which are six congruent, isosceles triangles) and has three different inter-atomic distances. To test the above arguments we computed the quality of five particle clusters in four dimensions, where the classical configuration of minimum energy is fully symmetric and there is no longer any frustration. Indeed, we found that the curve for the quality as a function of the polynomial power quantitatively agrees with the curves for three and four particle clusters in three dimensions.

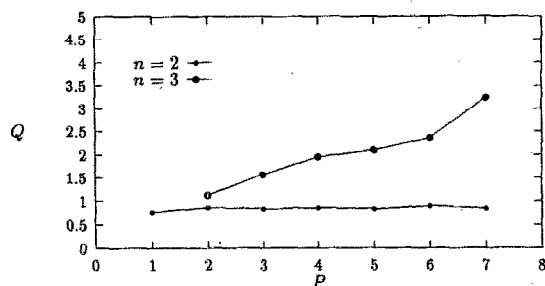


FIG. 6. Quality  $Q$ , a measure of the accuracy of the optimized trial function as defined in Eq. (6), as a function of power  $P$  of two- and three-body polynomials, labeled by  $n$ , for  $\frac{1}{2}\text{-Ne}_3$ .

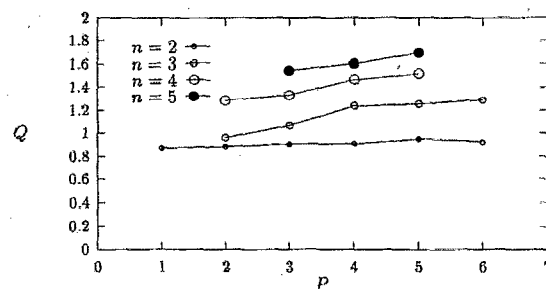


FIG. 8. Quality  $Q$ , a measure of the accuracy of the optimized trial function as defined in Eq. (6), as a function of power  $P$  of two-, three-, four- and five-body polynomials, labeled by  $n$ , for  $\frac{1}{2}\text{-Ne}_5$ .

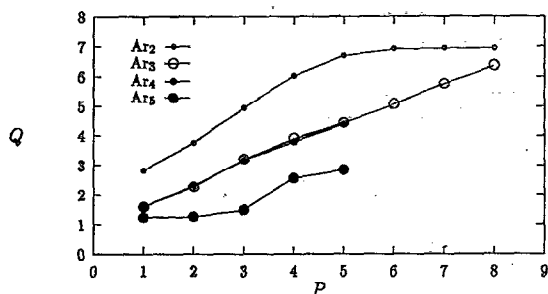


FIG. 9. Quality  $Q$ , a measure of the accuracy of the optimized trial function as defined in Eq. (6), as a function of power  $P$  of the complete polynomial for argon clusters of sizes two through five.

Note that for very accurate optimized trial functions, the computed variance of the local energy no longer decreases as more terms are added to the complete polynomial. A clear example of this is  $\text{Ar}_2$ , in Fig. 9. We attribute this to noisy behavior of the local kinetic energy caused by round-off errors in the numerical differentiation, which produce an effect of the order of magnitude observed. The data plotted in Figs. 1–8 were obtained from the relatively small samples that were also used to perform the parameter optimization. Only small differences were detected in those cases where we checked the variances obtained from these small samples against those obtained from extensive Monte Carlo runs. The data shown in Figs. 9–11 were obtained from long runs (see below for details).

Our most accurate numerical estimates for the energies of various small clusters are summarized in Table I. The results were obtained by standard variational Monte Carlo methods (see Appendix A) and appear under the heading  $E_{\text{vmc}}$  in Table I. The estimated averages were obtained from runs of about  $10^7$  Monte Carlo steps per atom. The energy auto-correlation time of the sampling algorithm was of the order of ten steps in these units. For comparison we included, under the heading  $E_{\text{dmc}}$ , the diffusion Monte Carlo results of Ref. 4, and the estimates of the harmonic approximation, under  $E_{\text{har}}$ . Also included in Table I are two esti-

mates of the systematic Rayleigh–Ritz variational errors in the results, and an estimate of the statistical, Monte Carlo errors. For the systematic errors we employ the inequalities given in Eqs. (7) and (8). As mentioned above, an estimate of the energy gap in the spectrum is required for the error estimate based on the second inequality, which provides a bound proportional to the variance  $\chi^2$  of the local energy rather than its standard deviation  $\chi$ . As an order of magnitude estimate of the gap, we employed the harmonic approximation, and for completeness the required eigenvalues of the Hessian matrix of the potential energy at the classical minimum are listed in Table II. We also mention in passing that the classical energies are  $E_0^{\text{class}} = -1, -3, -6, -9.103\ 852\ 415\ 707\ 556$  for  $N=2, \dots, 5$ ; all inter-atomic distances are equal to unity except for  $N=5$ , where the trigonal bipyramid has height 0.813 335 784 076 977 and as base an equilateral triangle with sides of length 1.001 453 524 076 903. The quantity  $Q''$  listed in the last of column Table I is a measure of the statistical error relative to the energy and is defined as in Eq. (6) with  $\chi$  replaced by the standard error of the Monte Carlo sample. The numerical values of the dimensionless inverse masses of the atoms we considered are listed in Table III.

We note that, with the exception of the larger clusters, the variational bias as measured by  $Q'$  is smaller than the statistical error measured by  $Q''$ , so that only for the larger clusters more accurate results can be obtained by diffusion Monte Carlo for a comparable amount of computational effort.

## V. DISCUSSION

We have presented a study of trial wave functions for small clusters. The trial functions were designed to satisfy the correct asymptotic behavior at small and large distances within the pair-correlation approximation. We demonstrated the computational tractability of wave functions that explicitly contain many-body contributions with the maximum number of interacting bodies for given cluster sizes and we obtained a quantitative measure of the importance of these contributions. As a measure of the quality we used  $Q$  as defined in Eq. (6). The estimate obtained from  $Q'$  in Eq. (9) is typically twice as high, but it relies on the gap computed

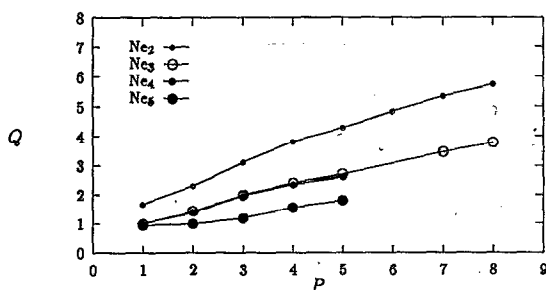


FIG. 10. Quality  $Q$ , a measure of the accuracy of the optimized trial function as defined in Eq. (6), as a function of power  $P$  of the complete polynomial for neon clusters of sizes two through five.

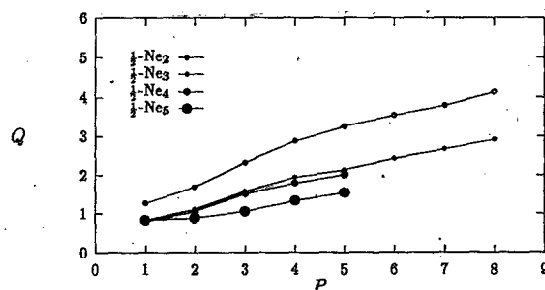


FIG. 11. Quality  $Q$ , a measure of the accuracy of the optimized trial function as defined in Eq. (6), as a function of power  $P$  of the complete polynomial for  $\frac{3}{2}$ -neon clusters of sizes two through five.

TABLE I. Variational Monte Carlo estimates of the ground state energies  $E_{\text{vmc}}$  of clusters containing up to five atoms compared with diffusion Monte Carlo estimates  $E_{\text{dmc}}$  taken from Ref. 4 and the harmonic approximation  $E_{\text{har}}$ . Standard errors in the last digit are given in parentheses. Estimates of the relative errors, as discussed in the text, are given by the quality estimators  $Q$  and  $Q'$  for the systematic variational errors and by  $Q''$  for the statistical errors. Also listed are estimates of the energy gap  $\Delta E_{\text{har}}$  between the ground state and the first excited state of the same symmetry. No statistical error is quoted for  $Q'$ : the dominant error in this case is the unknown error in  $\Delta E_{\text{har}}$ . In the column under the heading  $P$ , subsequent digits define the orders of the  $n$ -body polynomials used in wave functions.

	$N$	$P$	$E_{\text{vmc}}$	$E_{\text{dmc}}$	$E_{\text{har}}$	$\Delta E_{\text{har}}$	$Q$	$Q'$	$Q''$
Ar	2	8	-0.8489234312(1)	-0.8485(2)	-0.842	0.3166	6.93(8)	13.4	9.93(8)
	3	88	-2.553335364(1)	-2.555(1)	-2.532	0.3877	6.36(8)	11.9	9.36(8)
	4	555	-5.1182368(2)	-5.113(1)	-5.08	0.3166	4.37(7)	7.53	7.38(7)
	5	5555	-7.78598(1)	-7.791(1)	-7.73	0.2629	2.85(3)	4.23	5.84(3)
Ne	2	8	-0.566783279(1)	-0.5667(3)	-0.49	1.0105	5.73(5)	11.7	8.75(5)
	3	88	-1.7195589(3)	-1.721(1)	-1.5	1.2376	3.78(6)	7.40	6.78(6)
	4	555	-3.464174(8)	-3.461(1)	-3.1	1.0105	2.61(6)	4.67	5.61(6)
	5	5555	-5.29948(8)	-5.299(1)	-4.7	0.8391	1.80(4)	2.79	4.80(4)
$\frac{1}{2}$ -Ne	2	8	-0.427526736(31)	—	-0.3	1.4290	4.1(1)	8.77	7.1(1)
	3	88	-1.308443(2)	—	-0.9	1.7502	2.92(6)	5.95	5.94(6)
	4	555	-2.64356(3)	—	-1.8	1.4290	2.01(5)	3.74	5.02(5)
	5	5555	-4.0669(1)	—	-2.9	1.1867	1.55(6)	2.55	4.56(6)

obtained by the harmonic approximation. It is interesting to note in this context that in analogous computations for few-electron systems the bound  $\chi^2/\Delta E$  on the difference in energy between the variational and the ground state energies is often more than an order magnitude greater than the true difference.<sup>11</sup>

To deal with the many-body interactions we used bases of fundamental polynomial invariants, but we did not yet perform a systematic study of how to generate the computationally most efficient set of fundamental invariants. This holds in particular for larger systems where it is important to truncate the hierarchy of  $n$ -body contributions in a way that does not compromise the basic simplicity of the approach.

## ACKNOWLEDGMENTS

It is a great pleasure to acknowledge numerous discussions with David Freeman and Cyrus Umrigar without whose stimulating input this work would not have been done. This work was supported in part by the Office of Naval Research and in part by NSF Grants Nos. DMR-9214669, CHE-9203498, and PHY89-04035.

TABLE II. Harmonic approximation: eigenvalues  $\lambda_i$  of the Hessian matrix evaluated at the classical minimum energy configuration. The energy levels are given by  $E_{n_1, n_2, \dots} = E_0^{\text{class}} + \sum_i (n_i + 1/2) \sqrt{\lambda_i/m}$  with  $n_i = 0, 1, 2, \dots$ . The numbers in parentheses are multiplicities of the eigenvalues; the asterisks denote the lowest excited level that corresponds to a state with the same symmetry as the ground state, which defines the eigenvalue used to compute the gap  $\Delta E_{\text{har}}$  in Table I.

$N=2$	$N=3$	$N=4$	$N=5$
144 (*)	108 (2)	72 (2)	43.8795887067966 (2)
	216 (*)	144 (3)	99.3019911513688 (*)
		288 (*)	138.1042747649311 (2)
			148.5071864137867 (2)
			249.5948409655342 (1)
			307.1635684436352 (1)

## APPENDIX A: TRIAL FUNCTION OPTIMIZATION

To generate a sequence of configurations we used a standard Metropolis algorithm: starting from a given configuration the next one is constructed as follows. First, a new configuration is proposed by moving an atom  $i$  (selected at random) from  $\mathbf{r}_i^{\text{old}}$  to  $\mathbf{r}_i^{\text{pr}} = \mathbf{r}_i^{\text{old}} + \mathbf{d}$  where  $\mathbf{d}$  is a random vector sampled uniformly from a cube of with linear dimension  $d_0$  centered at the origin, chosen to give an acceptance of about 50%. The proposed configuration is accepted as the next configuration with probability

$$A_i = \min \left[ 1, \frac{|\Psi_T(\mathbf{R}^{\text{pr}})|^2}{|\Psi_T(\mathbf{R}^{\text{old}})|^2} \right], \quad (\text{A1})$$

otherwise the old configuration is kept as the next one.

This algorithm was used to generate the samples required for the optimization of the trial function, as discussed below, and also to compute the variational Monte Carlo estimates listed in Table I. We note that this particular version of the Metropolis algorithm is rather primitive and we expect that a version of the algorithm proposed by Umrigar<sup>12</sup> would be considerably more efficient. Since the emphasis of the current work is on the optimization of the wave function, the efficiency of the Monte Carlo sampling algorithm was of no great concern.

For the optimization of the trial wave function we minimize the variance of a fixed sample of  $s$  configurations (with  $s$  on the order of 100 configurations per parameter)  $\mathbf{R}_i$  sampled from  $|\Psi_T(\mathbf{R}, \mathbf{p}_0)|^2$ , where  $\mathbf{p}_0$  is an initial estimate of the parameters<sup>6</sup>. The variance is given by

TABLE III. Inverse dimensionless atomic mass  $\alpha = m^{-1}$ .

Ar	0.0006962
Ne	0.007092
$\frac{1}{2}$ -Ne	0.014184



TABLE IV. Coefficients  $C_{ijk}$  of the polynomial in the invariants  $I_{3,1}$ ,  $I_{3,2}$ , and  $I_{3,3}$  for a  $\text{Ne}_3$  cluster. The trial wave function is of the form of Eq. (27) with  $N=3$ ,  $\alpha=0.007\,092\,000$ ,  $r_0=1.1$ ,  $w=1.120\,918$ , and  $\gamma=0.907\,544\,158$ .

$C_{ijk}$	$(i,j,k)$
2.244 332	(2,0,0)
-1.512 491	(3,0,0)
-0.980 342	(4,0,0)
-0.981 160	(5,0,0)
-1.730 223	(6,0,0)
-3.759 748	(7,0,0)
-1.729 545	(8,0,0)
-2.742 988	(0,1,0)
2.191 407	(1,1,0)
1.950 623	(2,1,0)
0.412 871	(3,1,0)
2.180 581	(4,1,0)
14.877 507	(5,1,0)
2.827 592	(6,1,0)
-1.361 489	(0,2,0)
1.316 542	(1,2,0)
3.565 016	(2,2,0)
-23.619 189	(3,2,0)
1.027 512	(4,2,0)
-5.148 204	(0,3,0)
14.682 555	(1,3,0)
3.380 246	(2,3,0)
-9.469 800	(0,4,0)
32.051 098	(0,0,1)
19.134 118	(1,0,1)
12.411 076	(2,0,1)
49.151 573	(3,0,1)
11.797 876	(4,0,1)
41.574 293	(5,0,1)
25.096 391	(0,1,1)
-45.475 383	(1,1,1)
-27.791 103	(2,1,1)
11.415 828	(3,1,1)
58.250 660	(0,2,1)
-106.076 304	(1,2,1)
-318.164 801	(0,0,2)
404.995 936	(1,0,2)
-246.486 099	(2,0,2)
-520.003 142	(0,1,2)

$$\chi^2(\mathbf{p}) = \frac{\sum_i^s [\mathcal{E}(\mathbf{p}, \mathbf{R}_i) - \bar{\mathcal{E}}(\mathbf{p})]^2 W_i}{\sum_i^s W_i} \quad (\text{A2})$$

where re-weighting factors are defined as

$$W_i = \frac{|\Psi_T(\mathbf{p}, \mathbf{R}_i)|^2}{|\Psi_T(\mathbf{p}_0, \mathbf{R}_i)|^2} \quad (\text{A3})$$

and

$$\bar{\mathcal{E}}(\mathbf{p}) = \frac{\sum_i^s \mathcal{E}(\mathbf{p}, \mathbf{R}_i) W_i}{\sum_i^s W_i} \quad (\text{A4})$$

The optimization can be regarded as a least-squares parameter fit, for which the Levenberg–Marquardt algorithm can be used. If the initial estimate  $\mathbf{p}_0$  of the variational parameters is poor, in the sense that the variance of the weights  $W_i$  becomes large, the procedure is restarted, and a new set

TABLE V. Fundamental invariants for 4 particle clusters.

$I_{4,1}$	$x_{12} + x_{13} + x_{14} + x_{23} + x_{24} + x_{34}$
$I_{4,2}$	$x_{14}x_{23} + x_{13}x_{24} + x_{12}x_{34}$
$I_{4,3}$	$x_{12}^2 + x_{13}^2 + x_{14}^2 + x_{23}^2 + x_{24}^2 + x_{34}^2$
$I_{4,4}$	$x_{12}x_{13}x_{14} + x_{12}x_{23}x_{24} + x_{13}x_{23}x_{34} + x_{14}x_{24}x_{34}$
$I_{4,5}$	$x_{12}x_{13}x_{23} + x_{12}x_{14}x_{24} + x_{13}x_{14}x_{34} + x_{23}x_{24}x_{34}$
$I_{4,6}$	$x_{12}^3 + x_{13}^3 + x_{14}^3 + x_{23}^3 + x_{24}^3 + x_{34}^3$
$I_{4,7}$	$x_{14}^2x_{23} + x_{13}^2x_{24} + x_{12}^2x_{34}$
$I_{4,8}$	$x_{12}^4 + x_{13}^4 + x_{14}^4 + x_{23}^4 + x_{24}^4 + x_{34}^4$
$I_{4,9}$	$x_{12}^5 + x_{13}^5 + x_{14}^5 + x_{23}^5 + x_{24}^5 + x_{34}^5$

of configurations is sampled using the distribution defined by the wave function with the current, improved parameter estimates.

With the exception of the parameters  $w$  and  $r_0$  used in the definition of the inter-atomic distance variables  $\hat{r}_{ij}$ , defined in Eq. (24), all parameters appear linearly in the logarithm of the wave function. The latter can therefore be written in the form

$$\log \Psi_T(\mathbf{p}, \mathbf{R}) = \mathbf{A} \cdot \mathbf{f}(\mathbf{R}), \quad (\text{A5})$$

where  $\mathbf{A}$  is a parameter vector and  $\mathbf{f}$  is a conjugate vector of functions. These functions can be chosen to depend only on the configuration variables  $\mathbf{R}$ , but not the variational parameters (except  $w$  and  $r_0$ ). For a given sample of configurations, this way of writing the wave function allows one to perform the computationally expensive evaluation of the  $\mathbf{f}$  for each configuration in the sample no more than once for each parameter optimization. We note that variation of  $w$  and  $r_0$  would preclude this separation of configuration variables and parameters, but it was found that changes in  $w$  in the range from one to two could be compensated by changes in the parameters appearing in  $\mathbf{A}$  ranging from 10% to 20% without significant increase in the minimized variance of the local energy. Similarly, changes of  $r_0$  roughly from 1 to 1.2 have insignificant effects.

Finally, as a simple example included for those readers who would want to reproduce some of our results we tabulate in Table IV the optimized parameters for the  $\text{Ne}_3$  cluster. The trial function presented utilizes the complete two- and three-body polynomial expanded to order eight.

To calculate the kinetic energy we used Eq. (12). Since some of the numbers presented reflect the finite accuracy of the numerical derivatives we present some further detail here. For numerical evaluation of the second-order derivatives appearing in the kinetic energy we used three-point central difference scheme with finite difference  $\epsilon_2$  given by

$$\epsilon_2 = \max(|x|, 0.1) 10^{-d/4}, \quad (\text{A6})$$

where  $d=15$  is our machine floating point precision<sup>13</sup> and  $x$  is the point at which the derivative is computed. For the gradient we used a two-point scheme with

$$\epsilon_1 = 1.9 \max(|x|, 0.1) 10^{-d/3}. \quad (\text{A7})$$

This allows us to get relative numerical accuracy for the second-order derivatives of about  $10^{-7}$ . Of course, the factor 1.9 can be safely omitted, it is included to help the reader to reproduce our numerical result as close as possible. Also, we

TABLE VI. Fundamental invariants for 5 particle clusters. The second column gives the number of terms in the invariant to its right.

$I_{5,1}$	10	$x_{12} + x_{13} + x_{14} + x_{15} + x_{23} + x_{24} + x_{25} + x_{34} + x_{35} + x_{45}$
$I_{5,2}$	10	$x_{12}^2 + x_{13}^2 + x_{14}^2 + x_{15}^2 + \dots$
$I_{5,3}$	15	$x_{14}x_{23} + x_{15}x_{23} + x_{13}x_{24} + x_{15}x_{24} + \dots$
$I_{5,4}$	10	$x_{12}^3 + x_{13}^3 + x_{14}^3 + x_{15}^3 + x_{23}^3 + x_{24}^3 + x_{25}^3 + x_{34}^3 + x_{35}^3 + x_{45}^3$
$I_{5,5}$	10	$x_{12}x_{13}x_{23} + x_{12}x_{14}x_{24} + x_{12}x_{15}x_{25} + x_{13}x_{14}x_{34} + \dots$
$I_{5,6}$	20	$x_{12}x_{13}x_{14} + x_{12}x_{13}x_{15} + x_{12}x_{14}x_{15} + x_{13}x_{14}x_{15} + \dots$
$I_{5,7}$	30	$x_{14}^2x_{23} + x_{15}^2x_{23} + x_{14}^2x_{24} + x_{15}^2x_{24} + \dots$
$I_{5,8}$	5	$x_{12}x_{13}x_{14}x_{15} + x_{12}x_{23}x_{24}x_{25} + x_{13}x_{23}x_{34}x_{35} + x_{14}x_{24}x_{34}x_{45} + x_{15}x_{25}x_{35}x_{45}$
$I_{5,9}$	10	$x_{12}^4 + x_{13}^4 + x_{14}^4 + x_{15}^4 + x_{23}^4 + x_{24}^4 + x_{25}^4 + x_{34}^4 + x_{35}^4 + x_{45}^4$
$I_{5,10}$	10	$x_{15}x_{23}x_{24}x_{34} + x_{13}x_{14}x_{25}x_{34} + x_{12}x_{15}x_{25}x_{34} + x_{12}x_{14}x_{24}x_{35} + \dots$
$I_{5,11}$	15	$x_{14}^2x_{23}^2 + x_{15}^2x_{23}^2 + x_{13}^2x_{24}^2 + x_{15}^2x_{24}^2 + \dots$
$I_{5,12}$	15	$x_{13}x_{14}x_{23}x_{24} + x_{13}x_{15}x_{23}x_{25} + x_{14}x_{15}x_{24}x_{25} + x_{12}x_{14}x_{23}x_{34} + \dots$
$I_{5,13}$	30	$x_{12}^2x_{13}x_{23} + x_{12}^2x_{13}x_{23} + x_{12}^2x_{13}x_{23} + x_{12}^2x_{14}x_{24} + \dots$
$I_{5,14}$	30	$x_{14}^3x_{23} + x_{15}^3x_{23} + x_{14}^3x_{24} + x_{15}^3x_{24} + \dots$
$I_{5,15}$	10	$x_{12}^5 + x_{13}^5 + x_{14}^5 + x_{15}^5 + x_{23}^5 + x_{24}^5 + x_{25}^5 + x_{34}^5 + x_{35}^5 + x_{45}^5$
$I_{5,16}$	10	$x_{15}^2x_{23}x_{24}x_{34} + x_{13}x_{14}x_{25}x_{34} + x_{12}x_{15}x_{25}x_{34} + x_{13}x_{15}x_{24}x_{35} + \dots$
$I_{5,17}$	12	$x_{14}x_{15}x_{23}x_{25}x_{34} + x_{13}x_{15}x_{24}x_{25}x_{34} + x_{14}x_{15}x_{23}x_{24}x_{35} + x_{13}x_{14}x_{24}x_{25}x_{35} + \dots$
$I_{5,18}$	20	$x_{12}^2x_{13}x_{14}x_{15} + x_{12}^2x_{13}x_{14}x_{15} + x_{12}x_{13}x_{14}x_{15} + x_{12}x_{13}x_{14}x_{15} + \dots$
$I_{5,19}$	30	$x_{12}^2x_{13}x_{23} + x_{12}^2x_{13}x_{23} + x_{12}^2x_{13}x_{23} + x_{12}^2x_{14}x_{24} + \dots$
$I_{5,20}$	30	$x_{12}^2x_{13}x_{23} + x_{12}^2x_{13}x_{23} + x_{12}^2x_{13}x_{23} + x_{12}^2x_{14}x_{24} + \dots$
$I_{5,21}$	30	$x_{14}^4x_{23} + x_{15}^4x_{23} + x_{14}^4x_{24} + x_{15}^4x_{24} + \dots$
$I_{5,22}$	30	$x_{14}^2x_{15}x_{23} + x_{13}x_{15}x_{24} + x_{15}x_{23}x_{24} + x_{13}x_{14}x_{25} + \dots$
$I_{5,23}$	30	$x_{14}^3x_{23} + x_{15}^3x_{23} + x_{14}^3x_{24} + x_{15}^3x_{24} + \dots$
$I_{5,24}$	30	$x_{14}x_{15}x_{23}^3 + x_{15}x_{23}x_{24}^3 + x_{13}x_{15}x_{24}^3 + x_{14}x_{23}x_{25}^3 + \dots$

note that our scheme uses five points to approximate both derivatives. A five-point difference scheme might be used and yield more accurate results. We did not investigate this approach nor the analytic computation of derivatives.

## APPENDIX B: INVARIANTS

In Tables V and VI we list the fundamental invariants for clusters of four and five particles. Figure 12 is a graphical representation of the connectivity of the invariants. To construct a single monomial term of an invariant from a given diagram one labels the vertices from 1,2,...,N. Each pair of vertices  $i$  and  $j$  connected by  $l$  edges represents a factor  $\tilde{r}_{ij}^l$ . To get the full invariant, sum over all permutations of site labels with the restriction that different permutations yielding the same monomial are counted only once. The system for  $N=3$  is known to be complete. We have not attempted to prove that the systems given here form complete bases for  $N=4$  and  $N=5$ , but we have checked that the sets are complete up to and including polynomials order eight and five respectively. Also it is likely that systems can be constructed that are computationally superior and even have fewer fundamental invariants.

It should be noted the set for  $N=4$  has syzygies (polynomials in the invariants that vanish identically). For example, there are homogeneous polynomials of order eight that can be expressed in a one-parameter infinity of different ways as polynomials in the invariants. In practice this means for the trial functions that the coefficients of the polynomials in the invariants are not completely independent. Since the number of of redundant parameters is small, this causes no problem during the parameter optimization and we did not explore the syzygies systematically.

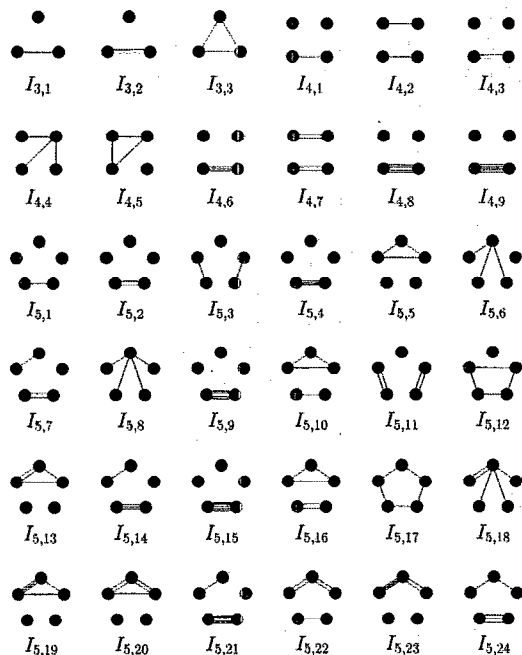


FIG. 12. Graphical representation of fundamental invariants for clusters of sizes  $N=3$ ,  $N=4$ , and  $N=5$ .

<sup>1</sup>V. R. Pandharipande, S. C. Pieper, and R. B. Wiringa, Phys. Rev. B **34**, 4571 (1986).

<sup>2</sup>M. V. Rama Krishna and K. B. Whaley, J. Chem. Phys. **93**, 746 (1990); **93**, 6738 (1990); Phys. Rev. Lett. **64**, 1126 (1990); Mod. Phys. Lett. B **4**, 895 (1990).

- <sup>3</sup>M. V. Rama Krishna and K. B. Whaley, *Z. Phys. D* **20**, 223 (1991).
- <sup>4</sup>S. W. Rick, D. L. Lynch, and J. D. Doll, *J. Chem. Phys.* **95**, 3506 (1991).
- <sup>5</sup>R. N. Barnett and K. B. Whaley, *Phys. Rev. A* **47**, 4082 (1993).
- <sup>6</sup>C. J. Umrigar, K. G. Wilson, and J. W. Wilkins, *Phys. Rev. Lett.* **60**, 1719 (1988), and in *Computer Simulation Studies in Condensed Matter Physics: Recent Developments*, edited by D. P. Landau, K. K. Mon, and H. B. Schüttler, Springer Proc. Phys. (Springer, Berlin, 1988); C. J. Umrigar, *Int. J. Quant. Chem. Symp.* **23**, 217 (1989). Minimization of the variance of the energy as means of optimizing trial wave functions goes back to the 1930s. The second paper contains pertinent references.
- <sup>7</sup>J. de Boer, *Physica* **139**, **149**, **510**, **520** (1948).
- <sup>8</sup>S. Goedecker and K. Maschke, *Phys. Rev. B* **44**, 10 365 (1991).
- <sup>9</sup>T. Kato, *Comm. Pure Appl. Math.* **10**, 151 (1957).
- <sup>10</sup>H. Weyl, *The Classical Groups* (Princeton University, Princeton, NJ, 1946); D. Cox, J. Little, and D. O'Shea, *Ideals, Varieties, and Algorithms* (Springer-Verlag, Berlin, 1991); B. Sturmfels, *Algorithms in Invariant Theory* (Springer-Verlag, Berlin, 1993).
- <sup>11</sup>C. J. Umrigar (private communication).
- <sup>12</sup>C. J. Umrigar, *Phys. Rev. Lett.* **71**, 408 (1993).
- <sup>13</sup>In C this constant  $d$  is conventionally called DBL\_DIG and can be found in a standard include header file called float.h.